arXiv:1611.07182v1 [cond-mat.mtrl-sci] 22 Nov 2016

Investigating resonance energy transfer from protein molecules to van der Waals nanosheets

Arun Singh Patel
School of Computational & Integrative Sciences, Jawaharlal Nehru University, New Delhi-110067, India[a)]
Praveen Mishra
School of Computational & Integrative Sciences, Jawaharlal Nehru University, New Delhi-110067, India
Pawan K. Kanaujia
Nanophotonics Laboratory, Department of Physics, Indian Institute of Technology Delhi, New Delhi-110016, India
Syed Shariq Husain
School of Computational & Integrative Sciences, Jawaharlal Nehru University, New Delhi-110067, India
G.Vijaya Prakash
Nanophotonics Laboratory, Department of Physics, Indian Institute of Technology Delhi, New Delhi-110016, India
Anirban Chakraborti
School of Computational & Integrative Sciences, Jawaharlal Nehru University, New Delhi-110067, India[b)]

(Dated: 23 November 2016)

The resonance energy transfer (RET) from tryptophan present in bovine serum albumin (BSA) to two dimensional (2D) nanomaterials has been reported. In these bio-nano systems, BSA molecules act as efficient donors while 2D van der Waals nanosheets of graphene, molybdenum disulfide (MoS_2) and tungsten disulfide (WS_2) act as acceptors. The fluorescence emission from tryptophan arises at 350 nm, in presence of 2D nanosheets, the fluorescence intensity of BSA decreases. The time resolved fluorescence study shows that there is decrease in the fluorescence lifetime of BSA molecules in presence of 2D nanosheets. The decrease in fluorescence lifetime of BSA confirms the energy transfer phenomenon in bio-nano interactions. This study is important for finding the bio-compatibility of 2D nanomaterials in biological applications.

In recent years, two dimensional (2D) nanosheets of van der Waals (vdW) materials have been extensively studied due to their intriguing optical, electronic, structural and chemical properties[1–5]. These materials include a wide range of nanomaterials – zero band gap to non-zero band gap. Among various types of vdW nanomaterials, graphene and transition metal dichalcogenides (TMDCs) nanosheets of the MX_2 type (M= Mo, W; X=S, Se, Te), are the most studied materials[6–9]. These materials have the advantage over other nanomaterials due to their high stability, high surface to volume ratio and a number of layer dependent electronic and optical properties[10–12]. Graphene consists of carbon atoms, arranged in a regular atomic-scale chicken wire (hexagonal) pattern. The emergence of graphene helped further the exploration of other two dimensional nanomaterials like, 2D sheets of TMDCs[13,14]. Among various TMDCs nanosheets, MoS_2 and WS_2 have been lately used in various optoelectronic devices. In bulk form, these TMDCs are found to be indirect band gap semiconductors, while for single layers, they are direct band gap semiconductors with different band gap energies[15–17], e.g., MoS_2 has 1.2 eV indirect band gap in bulk form, while for single layer it has direct band gap of 1.8 eV[18], and similarly, WS_2 has 1.4 eV indirect band gap in bulk form, while in case of single layer it is a 2.1 eV direct band gap semiconductor[19]. Recently, graphene as well as TMDC nanosheets have been used in resonance energy transfer (RET) phenomenon as acceptors of energy/charge[20–25]. The RET phenomenon is observed in various physical, chemical and biological systems[26,27]. In order to observe RET, one material acts as a donor and the other material as an acceptor of energy. Very recently, Sampat et al. has studied RET from quantum dots to MoS_2 nanosheets[20], Goodfellow et al. used CdSe/CdS QDs as donors and WS_2 nanosheets as acceptor in RET[24]. Similarly, Swathi et al. used a fluorescent dye as a donor and graphene as an acceptor for resonance energy transfer[28]. There are fewer studies on RET in biomolecules like protein and nanomaterials. Sen et al. have investigated RET in human serum albumin (HSA) protein molecules and gold nanoparticles[29]. Recently, Kuchlyan et al. have studied the interaction of BSA molecules with graphene oxide nanosheets[30]. Prior to application of nanomaterials in biological systems, testing the biocompatibility of the nanomaterials is essential. In this regard, the interaction of two dimensional nanosheets with biomolecules needs to be explored before their use in diagnosis and biomedical applications. The present study is important in the

[a)]Electronic mail: arunspatel.jnu@gmail.com
[b)]Electronic mail: anirban@jnu.ac.in

context of application of two dimensional nanosheets in bio-related fields, as for the first time here, we have investigated the bio-nano interaction in 2D nanosheets and bovine serum albumin molecules by means of resonance energy transfer.

In our study, the vdW nanosheets were synthesized by using the liquid exfoliation method. In a typical synthesis procedure, 50 mg of vdW powder (Sigma Aldrich) was dispersed in 10 mL of aqueous solution containing 10 mg BSA powder (Sigma Aldrich). Further the solution was ultrasonicated for 20 h using 25 W ultrasonication bath. After ultrasonication, the color of the solution changed, e.g., for MoS_2 from black to green, which confirmed the formation of nanosheets from bulk powder. Similarly, the color of WS_2 changed to brown, while that of graphene remained black. The supernatant was then collected and re-dispersed in water to prepare diluted stock solutions (0.05 mg/mL) of vdW nanosheets. The solutions were drop casted on silicon substrates and dried at room temperature for Raman spectroscopic studies. These nanosheets were characterized by transmission electron microscopy (TEM), Raman spectroscopy and absorption spectroscopy. The Raman spectra of graphene, MoS_2 and WS_2 nanosheets were recorded by Renishaw inVia confocal Raman spectrometer using 532 nm excitation source. For TEM study, the aqueous dispersions of the nanosheets were put on carbon coated copper grids and dried at room temperature. The TEM images of these nanosheets were recorded using JEOL-2010 TEM setup, which was operated at an accelerating voltage of 200 kV. The absorption spectra of these nanosheets were recorded using Shimadzu (UV-2450) UV-Vis spectrophotometer. In order to study RET in BSA and the van der Waals nanosheets, different quantities of nanosheets were mixed with a fixed quantity of BSA containing aqueous solution. All samples were prepared such that the amount of BSA molecules remains fixed (0.5 mg in 3.5 mL solution)in all sets, while only the quantities of the nanosheets were varied in different samples. All samples were incubated for 24 h to achieve equilibrium. The steady state fluorescence emissions of BSA, in absence and presence of nanosheets, were recorded using fluorimeter with excitation wavelength of 280 nm. The time resolved fluorescence study was performed using time correlated single photon counting (TCSPC) setup (FL920, Edinburgh Instruments, UK) with 284 nm light emitting diode as the excitation source.

The Raman spectra of the van der Waals nanosheets are shown in Fig. 1. Fig. 1a shows the Raman spectrum of graphene nanosheet. In case of graphene, three distinct Raman peaks are observed: 1350, 1582 and 2700 cm^{-1}; these peaks are known as D, G and 2D peaks, respectively[31]. D and G peaks originate due to the breathing modes of sp^2 carbon atoms in the ring and stretching of carboncarbon bonds respectively. The Raman spectrum of MoS_2 nanosheet is shown in Fig. 1b. There are two distinct Raman peaks: One at 385 cm^{-1} and the other at 405 cm^{-1}. These peaks arise due to in-plane and out-of-plane vibrations of S-Mo-S atoms, and are known as E^1_{2g} and A_{1g} vibrational modes, respectively[32]. In case of WS_2 nanosheets, E^1_{2g} and A_{1g} Raman peaks are observed at 351 cm^{-1} and 420 cm^{-1}, respectively.

The morphologies of two dimensional vdW nanosheets of graphene, MoS_2 and WS_2, were analyzed by transmission electron microscopy (TEM). Fig. 2a shows the TEM image of graphene nanosheets. The selective area electron diffraction (SAED) of graphene is shown in the inset of Fig. 2a. Similarly, the TEM images of MoS_2 and WS_2 are shown in Fig. 2b and Fig. 2c, respectively, and the insets of Fig. 2b and Fig. 2c show the SAED pattern of MoS_2 and WS_2 nanosheets, respectively.

The optical absorbance spectra of vdW nanosheets were recorded by the absorption spectrophotometer, and are shown in Fig. 3. The absorption spectrum of graphene shows an absorption peak around 280 nm. This absorption peak arises due to π-conjugation, which is partially restored within the graphene sheets. In case of MoS_2, two absorption peaks are observed; one at 620 nm and other at 670 nm. These peaks are the resultant of transitions between valence band and conduction band of MoS_2. The absorption peaks observed at 620 nm and 670 nm are assigned as B and A exciton peaks, respectively. Similarly, for WS_2 nanosheets the absorption peaks are observed at 530 nm and 630 nm. The absorption peaks are similar to the previous ones reported[33].

The interaction of these nanosheets with BSA molecules was studied by using fluorescence spectroscopic techniques. The steady state fluorescence spectra of BSA molecules in absence and presence of 2D nanosheets are recorded by fluorimeter using 280 nm excitation wavelength, and emission was recorded in wavelength range of 290-550 nm. The steady state fluorescence spectra of BSA molecules in presence of different concentration of 2D nanosheets are shown in Fig. 4. BSA shows fluorescence emission at 350 nm, which arises due to tryptophan present in BSA molecules[34]. In Fig. 4a, it is found that with increase in the concentration of graphene nanosheets, the fluorescence (Fl) intensity of BSA decreases. The decrease in Fl intensity confirms quenching due to graphene nanosheets. In Fig. 4b fluorescence quenching of BSA molecules in presence of MoS_2 nanosheets is shown. Similarly, for WS_2 nanosheets, the quenching of BSA fluorescence is shown in Fig. 4c. The fluorescence quenching of BSA molecules is confirmed, but in order to ascertain the quenching nature (static or dynamic), time resolved fluorescence study was done using time correlated single photon counting technique. It is observed that the fluorescence lifetime of BSA decays, in absence and presence of different concentrations of vdW nanosheets. The fluorescence lifetime decay spectra of BSA, in the absence and presence of 2D nanosheets, are shown in Fig. 5. Fig. 5a shows the Fl lifetime decay curve of BSA molecules in presence of graphene nanosheets. It is observed that with increase in the quantity of graphene, the fluorescence decay curves are

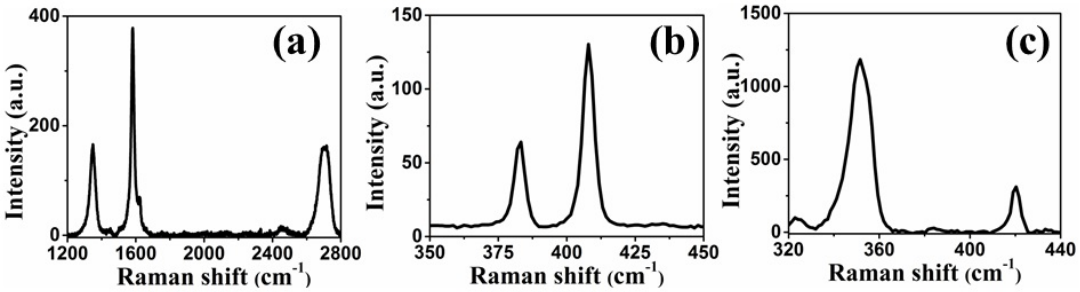

FIG. 1. Raman spectra of van der Waals nanosheets of (a) graphene, (b) MoS_2, and (c) WS_2.

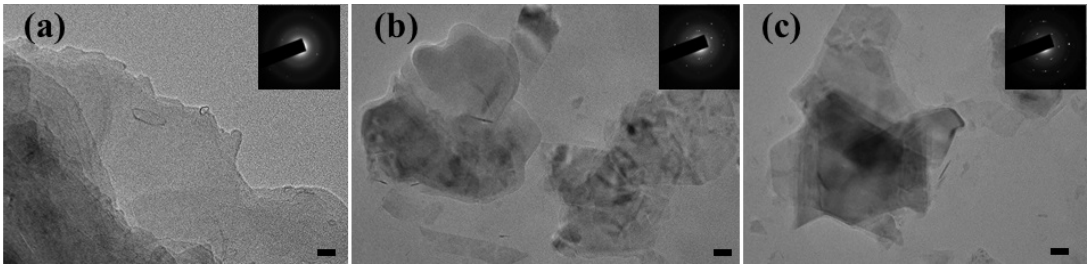

FIG. 2. TEM images of (a) graphene, (b) MoS_2, and (c) WS_2 nanosheets. Insets show selective area electron diffraction patterns of the respective 2D nanosheets.

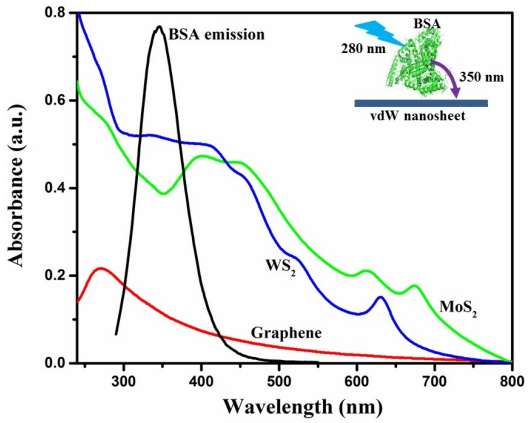

FIG. 3. Absorption spectra of graphene, MoS_2 nanosheets, and WS_2 nanosheets, along with the emission spectrum of BSA. Inset: Schematic representation of energy transfer between BSA and the van der Waals nanosheets.

steeper in comparison to pure BSA. There is a systematic change in the decay curves with increase in the quantity of graphene nanosheets. Similarly, Fig. 5b and Fig. 5c show the fluorescence lifetime decays of BSA, in presence of MoS_2 and WS_2 nanosheets, respectively. These decay curves were fitted with exponential decaying functions of following form[35]:

$$I(t) = \sum_{j=1}^{m} \alpha_j \exp(-t/\tau_j), \tag{1}$$

where m is the number of discrete decay components, τ_j are the decay times, and α_j represents the weighing parameter associated with the j^{th} decay. The decay curve of BSA in absence of nanosheets is fitted with bi-exponential ($m = 2$) decaying function, while in presence of nanosheets the curves are fitted with triple-exponential decaying function (fitted curves not shown). The average fluorescence lifetimes of BSA in absence, as well as in presence of nanosheets, were calculated using following equation[36]:

$$\langle \tau \rangle = \frac{\sum_{j=1}^{m} \alpha_j \tau_j}{\sum_{j=1}^{m} \alpha_j}. \tag{2}$$

The average fluorescence lifetime of pure BSA was found to be 6.41 ns. In presence of different quantities of graphene, the Fl lifetime decreases – for 0.1, 0.3, 0.5 and 0.7 mL of graphene solutions, the Fl lifetimes are found to be 6.08, 5.89, 5.66 and 5.55 ns, respectively. Thus, there is a systematic decrease in the Fl lifetimes of BSA molecules in presence of different quantities of graphene. Similarly, for MoS_2 nanosheets, the respective Fl lifetimes are found to be 6.39, 6.22, 5.70 and 5.62 ns in presence of 0.1, 0.3, 0.5 and 0.7 mL of MoS_2 nanosheets. For WS_2 the values are 6.26, 5.93, 5.61, 5.44 ns with 0.1, 0.3, 0.5 and 0.7 mL of WS_2 solutions, respectively. In all cases, with increase in the quantity of vdWs nanosheets, there is a corresponding decrease in the Fl lifetime of BSA molecules. In presence of 2D nanosheets, the fluorescence intensity as well as the fluorescence lifetime of BSA molecules are found to decrease. In Fig 6, variation of Fl intensity and Fl lifetime of BSA with different

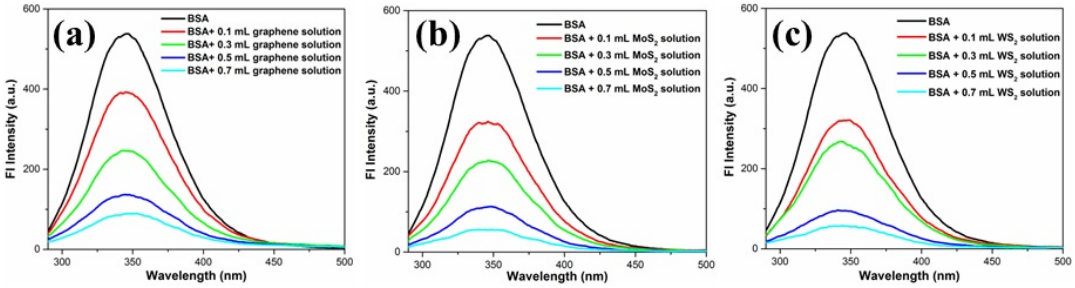

FIG. 4. Fluorescence spectra of BSA in absence and presence of different quantities of (a) graphene, (b) MoS_2, and (c) WS_2 nanosheets, respectively.

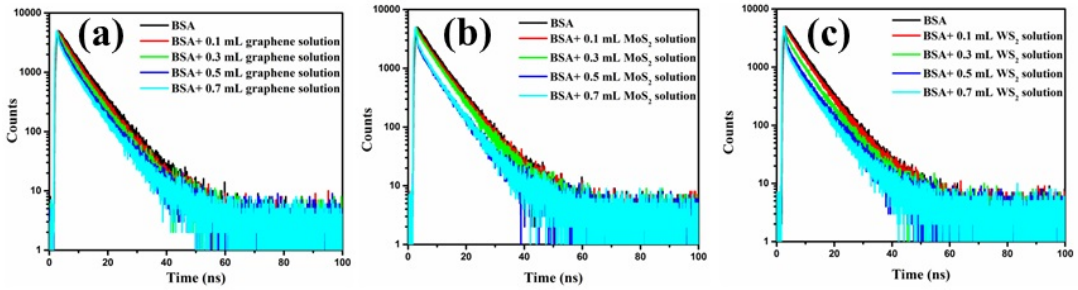

FIG. 5. Fluorescence lifetime decay curves of BSA, in the absence or in the presence of different quantities of (a) graphene, (b) MoS_2, and (c) WS_2 nanosheets, respectively.

quantities of 2D nanosheets are shown. The decrease in lifetime indicates that there is some energy transfer from the BSA molecules to 2D nanosheets. In Fig. 3, it is shown that the emission spectrum of BSA overlaps with the absorption spectra of vdW nanosheets. This results in transfer of some energy from BSA molecules to the nanosheets. In the process of energy transfer, the fluorophores show quenching in the Fl intensity, as well as Fl lifetimes. Using Fl lifetime data, the energy transfer efficiency from BSA molecules to 2D nanosheets has been calculated using following equation:

$$E = 1 - \frac{\tau_{DA}}{\tau_D}. \tag{3}$$

Here, τ_D and τ_{DA} are fluorescence lifetimes of BSA, in absence and presence of 2D nanosheets (acceptors), respectively. It is found that with increase in the concentration of acceptors the energy transfer efficiency increases. The energy transfer efficiencies, in case of graphene are found to be 5, 8, 12 and 13 % for 0.1, 0.3, 0.5 and 0.7 mL of graphene solutions, respectively. For MoS_2 the efficiencies are found to be 0.5, 3, 11 and 12 % with 0.1, 0.3, 0.5, and 0.7 mL of MoS_2 solutions, respectively. Finally, in the case of WS_2 nanosheets, the efficiencies were 2, 7, 12 and 15 % for 0.1, 0.3, 0.5 and 0.7 mL of the solutions, respectively.

The energy transfer efficiency was also calculated using steady state fluorescence emission data of BSA, in absence as well as presence of different vdWs nanosheets,

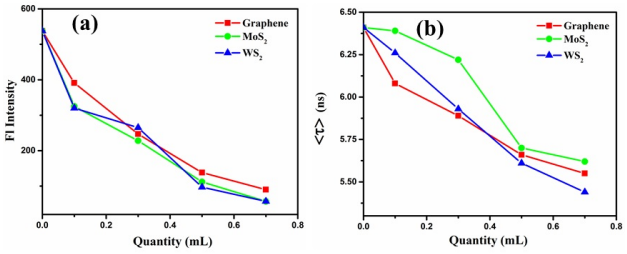

FIG. 6. Variation of: (a) fluorescence intensity and (b) fluorescence lifetime of BSA molecules, in presence of different quantities of 2D nanosheets.

using following equation:

$$E = 1 - \frac{F_{DA}}{F_D}, \tag{4}$$

where F_D is fluorescence intensity of BSA in absence of acceptors, while F_{DA} is intensity in presence of acceptors. The energy transfer efficiencies were found to be 27, 54, 74 and 83 % for 0.1, 0.3, 0.5 and 0.7 mL of graphene solutions, respectively. In case of MoS_2, the efficiencies were 40, 58, 79 and 89 % for 0.1, 0.3, 0.5 and 0.7 mL of MoS_2 solutions, respectively. Similarly, for WS_2, the efficiencies were found to be 40, 51, 82 and 89 % for 0.1, 0.3, 0.5 and 0.7 mL of the solutions, respectively.

There is a difference in the energy transfer efficiency values for Fl intensity data and Fl lifetime data, which indicates possibilities of two kinds of Fl quenching mech-

anisms, viz., static and dynamic. The decrease in fluorescence lifetimes normally corresponds to the dynamic nature of Fl quenching, and possibility of the resonance energy transfer from BSA to 2D nanosheets, while quicker decay in the Fl intensity confirms the static nature of quenching. In Fig. 3, it has been shown that the fluorescence emission of BSA molecules overlaps with some fraction of the absorption spectrum of the 2D nanosheets. The overlapping fluorescence of BSA and absorption of nanosheets causes transfer of energy from BSA molecules to the nanosheets. When the BSA molecules are excited by 280 nm excitation light, they emit at higher wavelength of 350 nm. In presence of nanosheets, some fraction of this emission gets absorbed by the nanosheets, which results in decrease in fluorescence intensity, as well as the fluorescence lifetimes of the BSA molecules. At the same time, the BSA molecules are attached to the nanosheets by van der Waals interaction and form BSA-nanosheets complexes, which is not fluorescent. Therefore, there is a steeper decrease in the fluorescence intensity of BSA molecules, in presence of nanosheets, as compared to decrease in the Fl lifetimes.

In summary, we have studied the resonance energy transfer between BSA molecules and two dimensional nanosheets of graphene, MoS_2 and WS_2. These nanosheets can be used as acceptors for energy transfer studied in biomolecules, which can be further explored to study the effect of 2D nanomaterials on biomolecules, prior to application of these nanomaterials in biological applications.

AC and ASP acknowledge financial support from grant number BT/BI/03/004/2003(C) of Government of India, Ministry of Science and Technology, Department of Biotechnology, Bioinformatics division. Authors thank the AIRF, JNU for TEM characterization and the FIST (DST, Govt. of India) UFO scheme of IIT Delhi for Raman/PL facility.

[1] W. Chen, E. J. Santos, W. Zhu, E. Kaxiras, and Z. Zhang, Nano Letters **13**, 509–514 (2013).
[2] H. Shi, H. Pan, Y.-W. Zhang, and B. I. Yakobson, Physical Review B **87**, 155304 (2013).
[3] K. F. Mak, K. He, C. Lee, G. H. Lee, J. Hone, T. F. Heinz, and J. Shan, Nature Materials **12**, 207–211 (2013).
[4] L. Falkovsky and S. Pershoguba, Physical Review B **76**, 153410 (2007).
[5] Y. Ding, Y. Wang, J. Ni, L. Shi, S. Shi, and W. Tang, Physica B: Condensed Matter **406**, 2254–2260 (2011).
[6] A. K. Geim and K. S. Novoselov, Nature Materials **6**, 183–191 (2007).
[7] B. Radisavljevic, A. Radenovic, J. Brivio, i. V. Giacometti, and A. Kis, Nature Nanotechnology **6**, 147–150 (2011).
[8] H. Ramakrishna Matte, A. Gomathi, A. K. Manna, D. J. Late, R. Datta, S. K. Pati, and C. Rao, Angewandte Chemie **122**, 4153–4156 (2010).
[9] Q. H. Wang, K. Kalantar-Zadeh, A. Kis, J. N. Coleman, and M. S. Strano, Nature Nanotechnology **7**, 699–712 (2012).
[10] H. Hibino, H. Kageshima, M. Kotsugi, F. Maeda, F.-Z. Guo, and Y. Watanabe, Physical Review B **79**, 125437 (2009).
[11] C. Lee, H. Yan, L. E. Brus, T. F. Heinz, J. Hone, and S. Ryu, ACS Nano **4**, 2695–2700 (2010).
[12] W. Zhao, R. M. Ribeiro, M. Toh, A. Carvalho, C. Kloc, A. Castro Neto, and G. Eda, Nano Letters **13**, 5627–5634 (2013).
[13] M. Chhowalla, H. S. Shin, G. Eda, L.-J. Li, K. P. Loh, and H. Zhang, Nature Chemistry **5**, 263–275 (2013).
[14] C. Zhang, Y. Chen, J.-K. Huang, X. Wu, L.-J. Li, W. Yao, J. Tersoff, and C.-K. Shih, Nature Communications **7** (2016).
[15] A. Chakraborti, A. S. Patel, P. K. Kanaujia, P. Nath, G. V. Prakash, and D. Sanyal, Physics Letters A **380**, 4057 – 4061 (2016).
[16] K. F. Mak, C. Lee, J. Hone, J. Shan, and T. F. Heinz, Phys. Rev. Lett. **105**, 136805 (2010).
[17] R. Ganatra and Q. Zhang, ACS Nano **8**, 4074–4099 (2014).
[18] J. Shakya, A. S. Patel, F. Singh, and T. Mohanty, Applied Physics Letters **108**, 013103 (2016).
[19] A. Berkdemir, H. R. Gutiérrez, A. R. Botello-Méndez, N. Perea-López, A. L. Elías, C.-I. Chia, B. Wang, V. H. Crespi, F. López-Urías, J.-C. Charlier, *et al.*, Scientific Reports **3** (2013).
[20] S. Sampat, T. Guo, K. Zhang, J. A. Robinson, Y. Ghosh, K. P. Acharya, H. Htoon, J. A. Hollingsworth, Y. N. Gartstein, and A. V. Malko, ACS Photonics **3**, 708–715 (2016).
[21] H. Zang, P. K. Routh, Y. Huang, J.-S. Chen, E. Sutter, P. Sutter, and M. Cotlet, ACS Nano **10**, 4790–4796 (2016).
[22] D. Kufer, T. Lasanta, M. Bernechea, F. Koppens, and G. Konstantatos, ACS Photonics (2016).
[23] D. Kufer, I. Nikitskiy, T. Lasanta, G. Navickaite, F. H. Koppens, and G. Konstantatos, Advanced Materials **27**, 176–180 (2015).
[24] K. M. Goodfellow, C. Chakraborty, K. Sowers, P. Waduge, M. Wanunu, T. Krauss, K. Driscoll, and A. N. Vamivakas, Applied Physics Letters **108**, 021101 (2016).
[25] F. Prins, A. J. Goodman, and W. A. Tisdale, Nano Letters **14**, 6087–6091 (2014).
[26] P. R. Selvin, Nature Structural Biology **7**, 730–734 (2000).
[27] K. Shankar, X. Feng, and C. A. Grimes, ACS Nano **3**, 788–794 (2009).
[28] R. Swathi and K. Sebastian, The Journal of Chemical Physics **130**, 086101 (2009).
[29] T. Sen, S. Mandal, S. Haldar, K. Chattopadhyay, and A. Patra, The Journal of Physical Chemistry C **115**, 24037–24044 (2011).
[30] J. Kuchlyan, N. Kundu, D. Banik, A. Roy, and N. Sarkar, Langmuir **31**, 13793–13801 (2015).
[31] W. Zhao, M. Fang, F. Wu, H. Wu, L. Wang, and G. Chen, Journal of Materials Chemistry **20**, 5817–5819 (2010).
[32] L. Yang, X. Cui, J. Zhang, K. Wang, M. Shen, S. Zeng, S. A. Dayeh, L. Feng, and B. Xiang, Scientific Reports **4** (2014).
[33] T. P. Nguyen, W. Sohn, J. H. Oh, H. W. Jang, and S. Y. Kim, The Journal of Physical Chemistry C **120**, 10078–10085 (2016).
[34] N. Tayeh, T. Rungassamy, and J. R. Albani, Journal of Pharmaceutical and Biomedical Analysis **50**, 107–116 (2009).
[35] A. S. Patel, H. Sahoo, and T. Mohanty, Applied Physics Letters **105**, 063112 (2014).
[36] A. S. Patel, H. Sahoo, and T. Mohanty, Journal of Fluorescence **26**, 1849–1855 (2016).